

Klaus Richter, Berlin University of Technology, email: klaus.richter@mac.com

ISO-CIE trend for the description of colour threshold data by new coordinates based on the device independent elementary colour coordinates of the report CIE R1-47:2009.

http://130.149.60.45/~farbmetrik/CIE_ISO_10.PDF

Version 1.2, 18 pages, 500 KB

Abstract:

The report CIE R1-47:2009 "Hue Angles of Elementary Colours" recommends the CIELAB hue angles $h_{ab} = 26, 92, 162, \text{ and } 272$ degrees for the elementary colors Red R , Yellow J , Green G , and Blue B . The dominant wavelength of these colours are approximately $\lambda_d = 494c, 575, 515, \text{ and } 475\text{nm}$. The different wavelength ranges defined by the four dominant wavelength are used to calculate the CIE data of six optimal colours. These colours $OYLCMV$ (names according to ISO/IEC 15775) have special properties. They are located on a triangle with OLV at the corners in the CIE (x, y) chromaticity diagram and on a hexagon in a chromatic value diagram (A, B) . The diagram (A, B) has a symmetry compared to the origin (white) for any CIE illuminant. This property of the coordinates A and B and the radial chromatic value C is the basis to describe the equal threshold for complementary optimal colours published by *Holtzmark* and *Valberg* (1969). One complementary colour series is for example $Y - W - V$ (Yellow - White - Violet blue) on lines in the diagrams (x, y) and (A, B) . Yellow Y and Violet Blue V have the same radial chromatic value C . It happens that the wavelength limits 380 to 515 nm and 515 to 770 nm of the two optimal colours have approximately the two dominant wavelength $\lambda_d = 475$ nm for Blue B and 575 nm for Yellow J . Therefore the series $Y - W - V$ is identical to the series $J - W - B$. An improved colour metric is discussed for the description of the colour threshold for complementary optimal colours and the elementary colours Red R and Green G .

1. Introduction: Elementary colours $RJGB$ and applications in image technology

The report CIE R1-47:2009 "Hue Angles of Elementary Colours" recommends the CIELAB hue angles $h_{ab} = 26, 92, 162, \text{ and } 272$ degrees for the elementary colors Red R , Yellow J , Green G , and Blue B . These hue angles are identical to the CIELAB hue angles of the CIE test colours no. 9 to 12 which are defined in CIE 13.3 to specify colour rendering properties of light sources.

Based on a request of ISO TC 159/SC4/WG2 "Ergonomic - Visual Display Requirements", CIE Division 1 "Vision and Colour" decided in 2008 a reportership by *Thorstein Seim (Norway)* to produce the report CIE R1-47. For the rgb -input data 100, 110, 010, and 001 this report allows to produce the four elementary hues $RJGB$ and any intermediate hue on any colour device.

The device independent hue output of the four elementary colours $RJGB$ compared to the six device colours $OLYLCVM$ (colour names according to ISO/IEC 15775) is shown for a standard offset process (*ORS18a*), a standard CRT monitor (*TLS00*), a photo printer (*PRS06a*) and the Swedish *NCS* system (*NRS11a*) for CIE standard illuminant D65 in the PDF file

<http://130.149.60.45/~farbmetrik/JE45/JE45L0NP.PDF>

For example for the standard offset process (*ORS18a*) the device color Violet blue V with the rgb -input value 001 has the CIELAB hue angle 305 degree. The colour of this hue angle appears very reddish compared to the elementary colour with the hue angle of 272 degree. The elementary hue B can be mixed by equal amounts of the colours V and C . ISO TC 159/SC4/WG2 requests to produce the elementary hue B instead of the device hue V on any colour device.

A new German standard series DIN 33872-1 to -6 (in print) specifies the output properties of printers and displays. Equally spaced visual output for equally spaced rgb -input color data and elementary hue output according to CIE R1-47 is recommended, see many DIN-test charts at

<http://www.ps.bam.de/33872E>

Therefore the development of an improved colour metric for colour thresholds based on elementary colours is an important step for many image technology applications.

2. Equal hue discrimination of complementary optimal colours

There is a visual phenomena that complementary optimal colours produced by a positive and negative mask with a prism (or grid) produce a similar discrimination at corresponding locations within both spectra. This indicates a high symmetry in vision and is one source for an improved colour vision model and improved formulas for the description of colour threshold, for example within the Technical Committee CIE TC1-63 “Validity of the range of CIE DE2000”. The CIE colour difference formula CIE DE2000 has been developed for colour differences in the range 1 to 5 CIELAB and fails to a high degree at threshold, see *Melgosa* (2009).

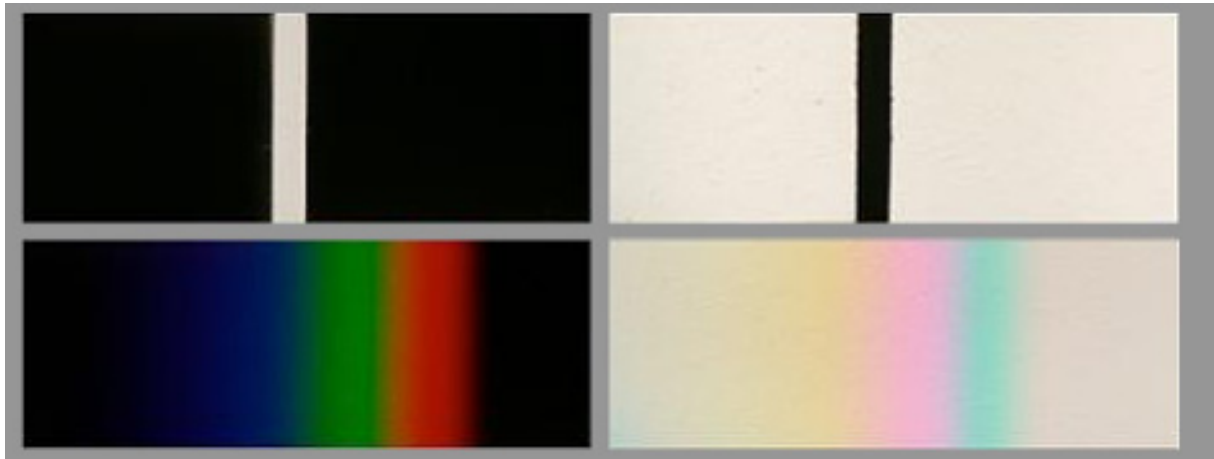


Fig. 1: Complementary optimal colours produced by a positive and negative mask with a prism
Fig. 1 shows optimal colours which are produced by a mixture of spectral colours between two wavelength limits. The visible spectrum is in the range between 400 nm and 700 nm. If the wavelength range produced by the positive or negative mask is about 100 nm then we see in Fig. 1 (*left*) three basic colours *O*, *L*, and *V* (Orange red, Leaf green, and Violet blue according to ISO/IEC 15775) and in Fig. 1 (*right*) three complementary colours *C*, *M*, and *Y* (Cyan blue, Magenta red, and Yellow).

There is the visual phenomena, that the visual hue discrimination is equal for the two colour series *OLV* and *CMY* for corresponding locations. This is approximately true for any mask and with any slit width.

Holtsmark and *Valberg* (1969) have measured the hue discrimination of optimal colours by a spectral colour integrator. In a white surround with two equal masks two beams have produced two equal half partite central fields of about 2 degree diameter. The location of one mask has to be moved until a hue threshold was visible. The same was done by an inverse masks and for six observers. The summary of the results produce the statement: The hue discrimination is equal with a negative and positive mask. The colour change is mainly defined by a hue and not by a luminance factor difference ΔY . The difference ΔY may be below threshold for all wavelength and the perceived hue difference may depend only on two chromatic differences ΔA in red-green and ΔB in blue-yellow direction. Appropriate chromatic value coordinates (*A*, *B*) are given in Fig. 17 and 19. For six optimal colours *OYLCVM* the CIE data are given in Fig. A.1 of Annex A. Annex B and C show a possible metric and 2 line elements for the description of the *Holtsmark-Valberg* results. In addition the formulas may be important for other additive colour systems, for example a CRT, a LCD or a LED monitor in image technology.

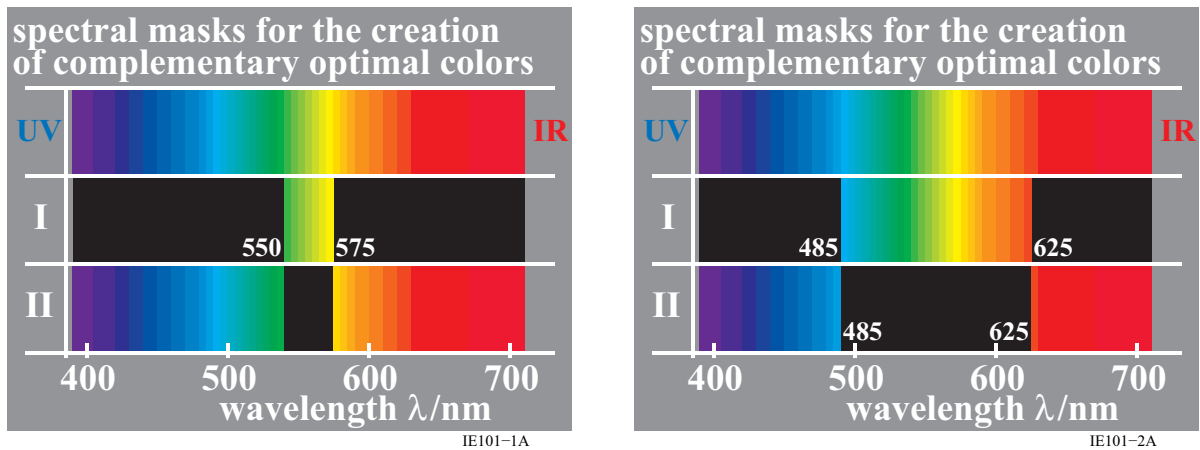


Fig. 2: Positive (I, top) and negative (II, down) mask to produce complementary optimal colours in a white surround (third beam with no mask).

Fig. 2 shows the spectral wavelength mixture for the positive and negative slit. Fig. 2 shows different slit width: a small (*left*) and a broad band wavelength range (*right*) The slit width did not change the result which are similar for the six observers (including myself) and all with normal colour vision. In the experiments of *Holstmark* and *Valberg* (1969) a xenon arc was used. The correlated colour temperature was about 6500 K and the luminance about 150 cd/m² for the white surround which corresponds to an illumination of 500 lux.

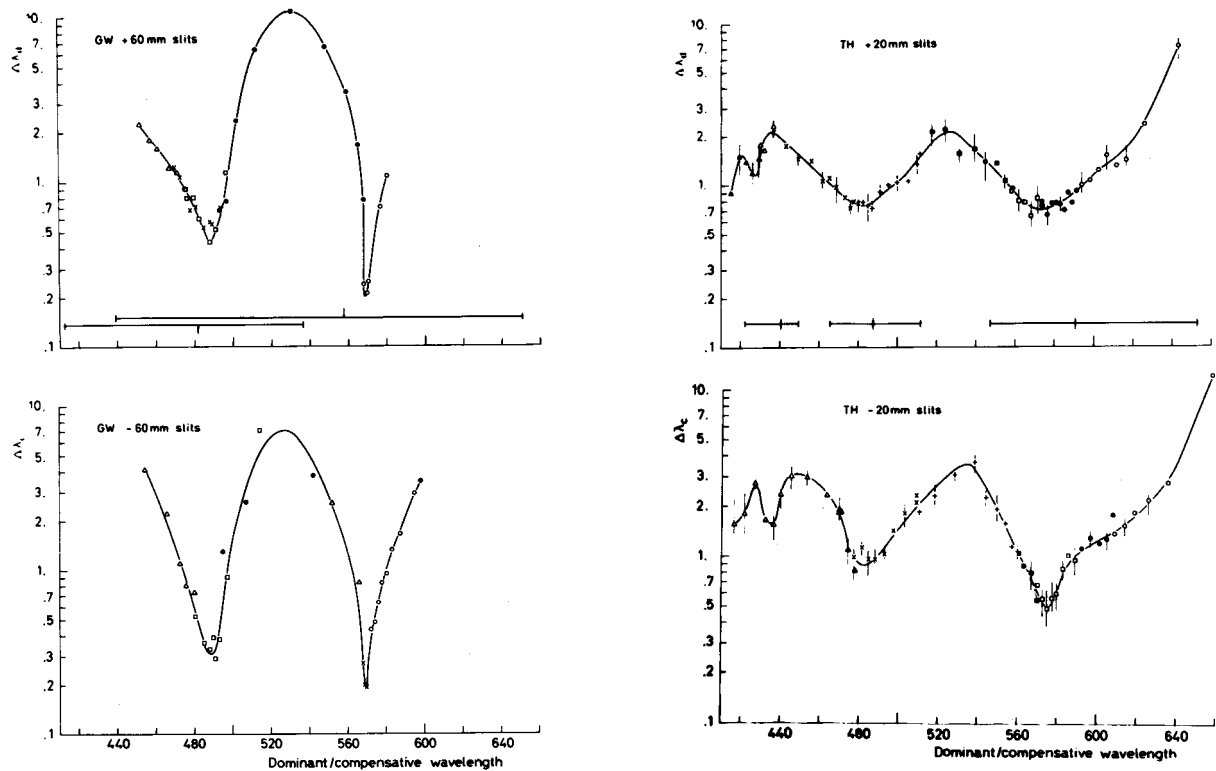


Fig. 3: Wavelength discrimination for complementary optimal colours for a broad band (60 mm) and a small band (20 mm) slit.

Fig. 3 shows examples for the experimental wavelength discrimination. The agreement is high according to *Holtsmark* and *Valberg* (1969) for the positive and negative slit and for broadband

(60 mm) and small band (20 mm) wavelength ranges. The spectrum (400 nm to 700 nm) covers about 100 nm. Therefore in Fig. 3 the slit width is about 60% and 20% of the spectrum.

3. CIE chromatic value functions $a_{\text{bar}}(\lambda)$ and $b_{\text{bar}}(\lambda)$ and colour vision model of *Hurvich and Jameson (1955)*

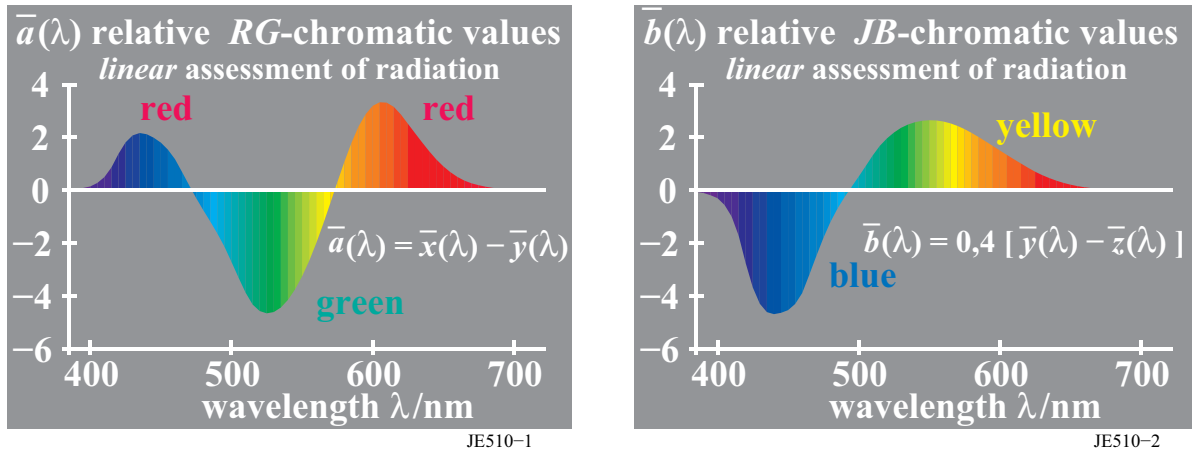


Fig. 4: *RG*- and *JB*-chromatic value function of *Hurvich* and *Jameson (1955)*.

Fig. 4 shows the *RG*- and *JB*-chromatic value functions of *Hurvich* and *Jameson (1955)*. Both are linear transformations of the CIE tristimulus value functions $x_{\text{bar}}(\lambda)$, $y_{\text{bar}}(\lambda)$, and $z_{\text{bar}}(\lambda)$. They indicate the spectral weighting of both either red or green and either blue or yellow. The zero points are near 475nm and 575nm for the read-green function (*left*) and near 500 nm for the yellow-blue function. Therefore the elementary hues *B*, *G*, and *J* shall be near the wavelength 475nm, 500nm, and 575nm. At least for Green *G* there is a deviation towards about 513nm instead of 500 nm, see later.

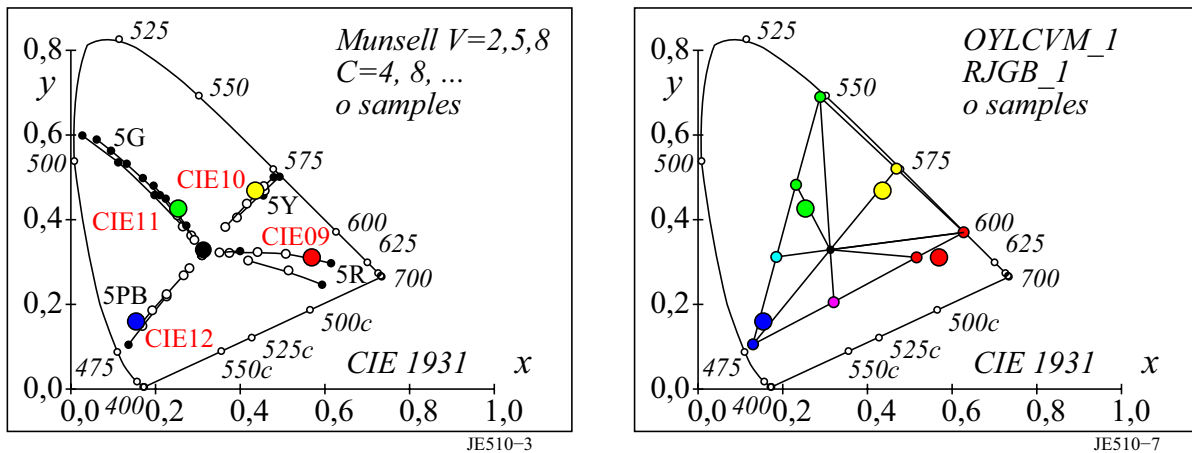


Fig. 5: CIE test colours no. 9 to 12 (*RJGB*) compared to colours of the *Munsell* colour order system (*left*) and six optimal colours *OYLCVM* of image technology (*right*).

Fig. 5 shows the CIE test colours no. 9 to 12 which appear elementary Red *R*, Yellow *J*, Green *G*, and Blue *B* (*RJGB*) according to the report CIE R1-47:2009 (*left*). In addition the real (o) and extrapolated colours of the *Munsell* colour order system are shown for Value 2, 5, and 8. The CIE test colours have approximately the hues 5*R*, 5*Y*, 5*G*, and 5*PB* of the *Munsell* colour order system. The three colours *O*, *L*, *V* and the additive mixture colours *C*, *M*, *Y* (names according to ISO/IEC 15775) are located on a triangle in the CIE (*x*, *y*) chromaticity diagram. The complementary colour series *O* - *W* - *C*, *L* - *W* - *M*, and *V* - *W* - *Y* are located on lines through the chro-

maticity of White W . This property is true for any affine transformation of chromaticity diagrams, for example the CIE (x, y) and the CIE (u', v') chromaticity diagram. Elementary Blue B and Yellow J are approximately on the line $V - W - Y$. The elementary colour Red R may be produced by the mixture $R = 0,18M$ and $0,82 O$ and the elementary colour Green G may be produced by the mixture $G = 0,3 C$ and $0,7 L$, compare data in Fig. A.1 of Annex A.

4. Optimal colours $O, L,$ and V and complementary colours $C, M,$ and Y in image technology and relation to the elementary colours $RJGB$

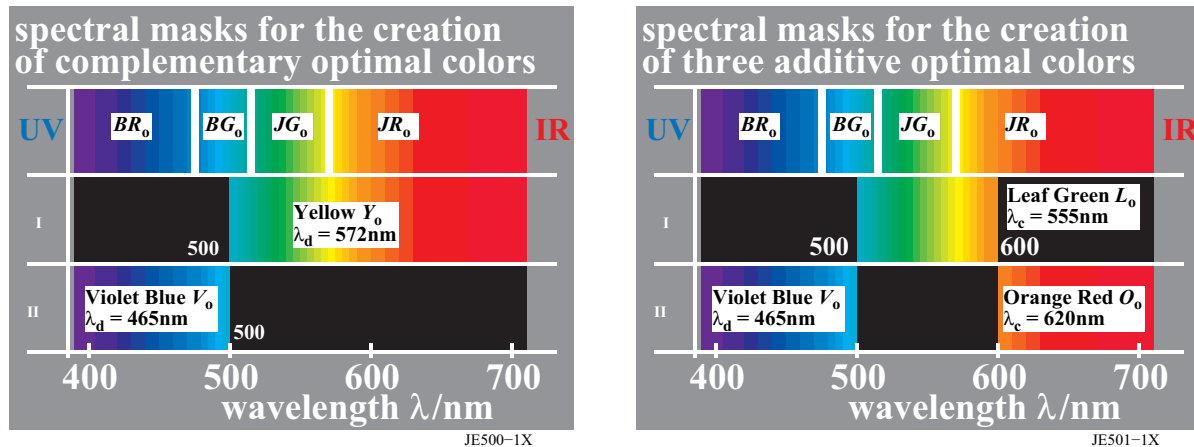


Fig. 6: Colours $V_o, L_o,$ and O_o and the mixture $Y_o = L_o + O_o$ often used in image technology. Fig. 6 shows the colours $V_o, L_o,$ and O_o and the mixture colour $Y_o = L_o + O_o$ which is often used in image technology (Index o = optimal colour). In Fig. 6 the limits of the wavelength range of Y_o and V_o do not match to the visual ranges which determine the optimal colours $BR_o, BG_o, JG_o,$ and JR_o . This match is done in the next Fig. 7. Again the colours OLV are located on a triangle in the CIE chromaticity diagram and the Yellow Y_o is located on a line between O_o and L_o , compare Fig. 5.

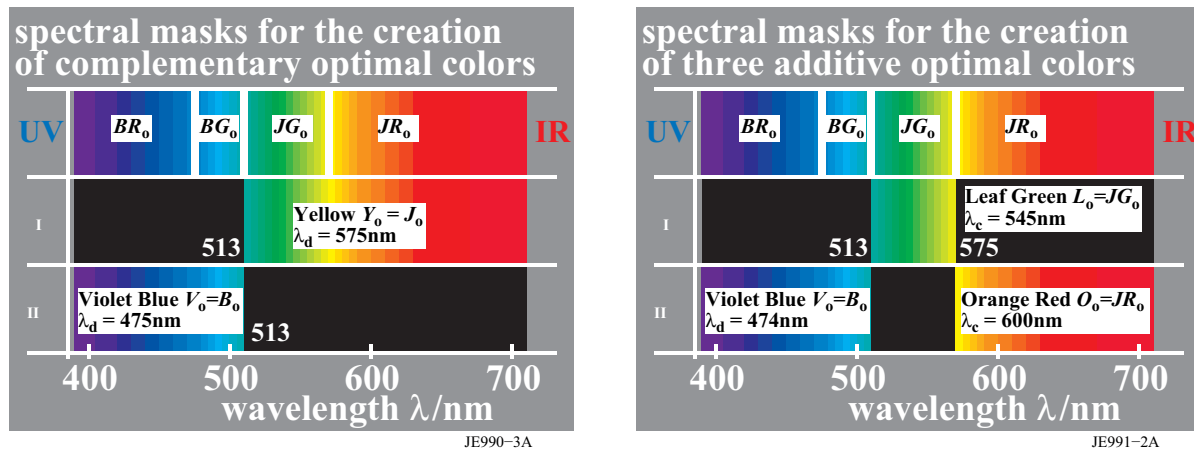


Fig. 7: Colours $V_o, L_o,$ and O_o and the mixture $Y_o = L_o + O_o = JG_o + JR_o$. Fig. 7 shows the colours $V_o, L_o,$ and O_o and the mixture $Y_o = L_o + O_o = JG_o + JR_o$. The limits of the wavelength ranges do now match to the visual ranges which determine $BR_o, BG_o, JG_o,$ and JR_o . For example Blue B_o and Yellow J_o are now defined by $B_o = V_o = BR_o + BG_o,$ and $J_o = Y_o = JG_o + JR_o$. Again all are located on a triangle in the CIE chromaticity diagram. However, Leaf green L_o with the wavelength limits of 513 nm and 575 nm is different compared to the wavelength limits 475 nm and 575 nm of Green G_o as expected by *Hurvich and Jameson (1955)*. The colour L_o appears yellow-green (here named JG_o).

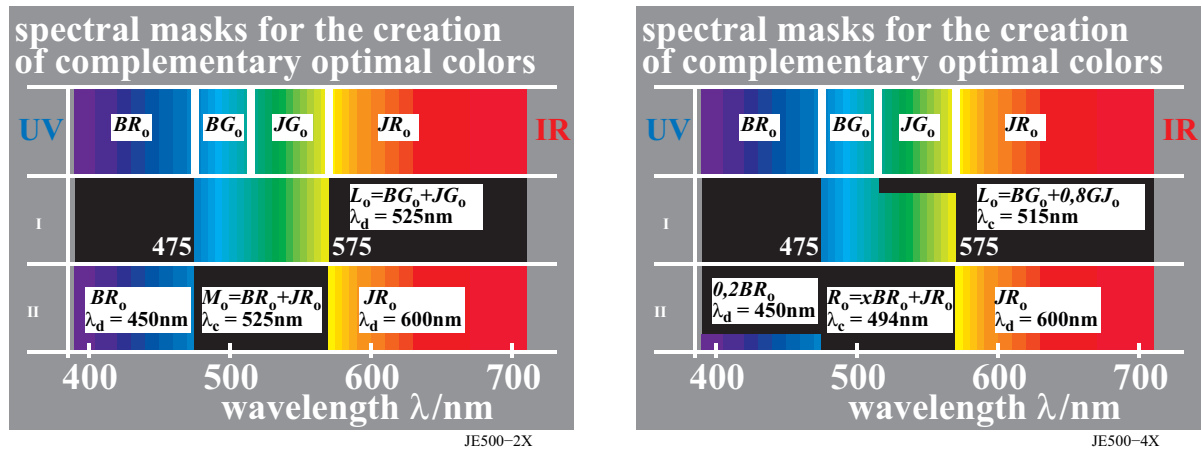


Fig. 8, Optimal colour L_o and complementary colour M_o (left) and a mixture colour elementary Green G and Red R (right) which both are mixed by two optimal colours of different ratio. Fig. 8 shows the optimal colour L_o and the complementary colour M_o (left) and mixture colour of elementary Green G and Red R (right) which both are mixed by two optimal colours of different ratio. Both are no optimal colours (no index o). According to the colour vision theory of *Hurvich* and *Jameson* (1955) in the left part the optimal colour L_o shall be elementary Green G_o and the complementary colour M_o elementary Red R_o , compare Fig. 4. Experiments show that a special mixture of BG_o and JG_o produces elementary Green G and a special mixture of BR_o and JR_o produce elementary Red R . Both are not any more optimal colours with a reflection of one in the whole wavelength range. It is approximately valid: $G_o = BG_o + 0,8 JG_o$ and $R_o = 0,2 BR_o + JR_o$. In addition it happens that the complementary colour of BG_o is elementary Red R_o with the dominant wavelength $\lambda_d = 494c$ nm. This Red R_o is again a optimal colour.

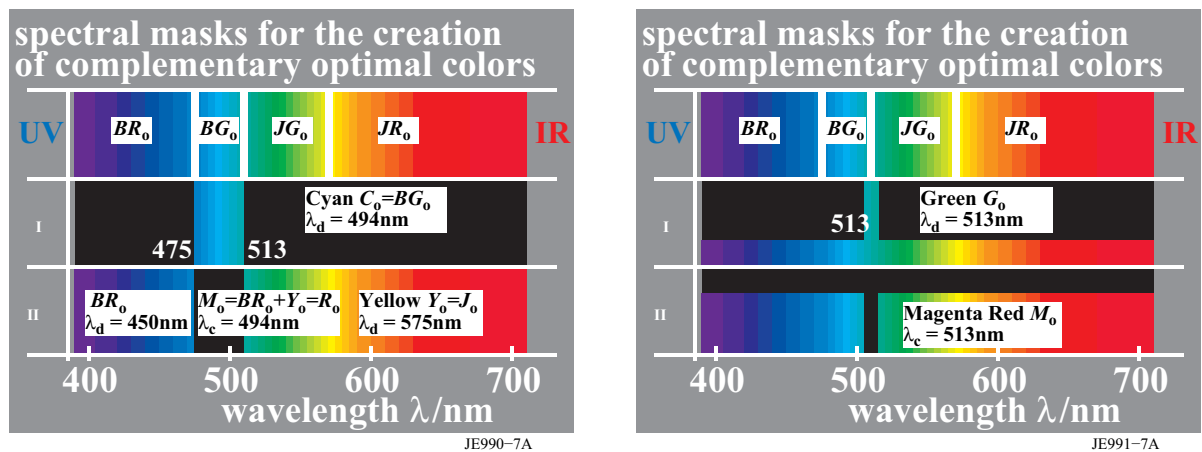


Fig. 9: Cyan Blue $C_o = BG_o$ and complementary colour which appears approximately elementary Red R_o (left); mixture of monochromatic Green G_o with about 30% of the complementary colour Magenta red M_o (right) and complementary colour (both mixtures no optimal colours). Fig. 9 shows Cyan blue $C = BG_o$ and the complementary colour which happens to appear elementary Red R_o . The Cyan blue C has the small band wavelength range 475 nm to 513 nm and the dominant wavelength $\lambda_d = 494$ nm. The complementary colour has the complementary wavelength $\lambda_c = 494c$ nm and this defines a broadband elementary Red $R_o = BR_o + JG_o + JR_o$. We know already from Fig. 8 that the wavelength range 475nm to 575nm produces a yellowish green. However, an elementary optimal colour Green G_o has the wavelength range 475nm to 550nm and the dominant wavelength 513nm which is the border between BG_o and JG_o .

If the colours at the ends of the spectrum BR_o and JR_o are excluded then the dominant wavelength is usually approximately in the middle of the wavelength range, for example $\lambda_d = 525$ nm is in the middle of the wavelength range 475 nm to 575 nm, compare Fig. 8 (left). This symmetry seems a main property of colour vision. If one mixes a monochromatic light with the complementary light “White minus Monochromatic”, then the hue appearance is approximately constant, compare Fig. 9 (right) In the CIE (x, y) chromaticity diagram all mixtures are located on a line between the chromaticity of white and the monochromatic colour. This indicates the same chromatic weighting function at both sides of the monochromatic wavelength. We know that the spectral luminance efficiency $V(\lambda)$ is to a high degree symmetric. The maximum value of $V(\lambda)$ is 100% at a wavelength near 550nm and has a value of 1% near both the wavelength 400nm and 700nm. The chromatic symmetry suggests that the chromatic coordinates are independent of $V(\lambda) = y_{bar}(\lambda)$. Therefore $a_{bar}(\lambda) = x_{bar}(\lambda) - y_{bar}(\lambda)$ for the red-green direction and $b_{bar}(\lambda) = -0,4 [z_{bar}(\lambda) - y_{bar}(\lambda)]$ for the yellow-blue direction is an appropriate choice. The factor -0,4 defines a lower weighting for the yellow-blue direction and the minus sign moves yellow at the top. The factor 0,4 is larger for the 10 degree viewing field and changes to 1% (0,01) near a 0,1 degree viewing field, This visual property is called small field tritanopia which suggest no yellow-blue discrimination near a 0,1 degree visual field. In an improved model the function $b_{bar}(\lambda)$ shall have the zero point near 513nm instead of 500nm.

5. Cone sensitivities $P(\lambda)$, $D(\lambda)$, $T(\lambda)$, and $V(\lambda)$, and $V'(\lambda)$ on a linear and logarithmic scale

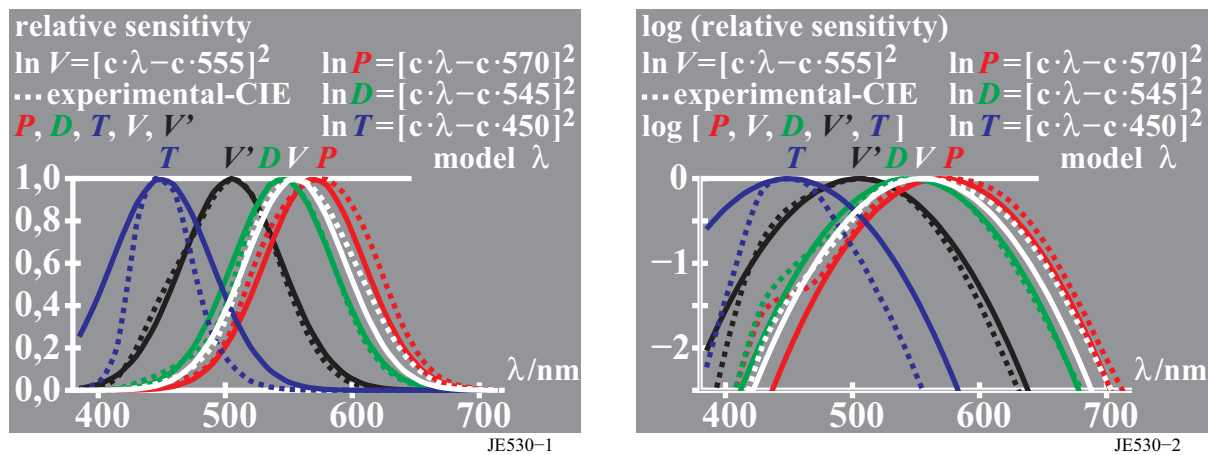


Fig. 10: Spectral sensitivities $P(\lambda)$, $D(\lambda)$, and $T(\lambda)$ of the cones PDT including $V(\lambda)$ and $V'(\lambda)$ on a linear and a logarithmic scale (left and right).

Fig. 10 shows the spectral sensitivities of the cones PDT (or LMS) according to the colour vision deficiencies Protanopia, Deuteranopia and Tritanopia which each miss one of the three sensitivities. In addition the spectral sensitivities for photopic and scotopic vision $V(\lambda)$ and $V'(\lambda)$ are shown. The model functions of parable shape show a good approximation of experimental data except for $T(\lambda)$ which produces a broader sensitivity in the model compared to experimental data. In summary the functions are approximately all shifted by the top wavelength and have all a similar shape. Therefore the log difference of two sensitivities form a line as function of wavelength. This is shown and discussed further in the following.

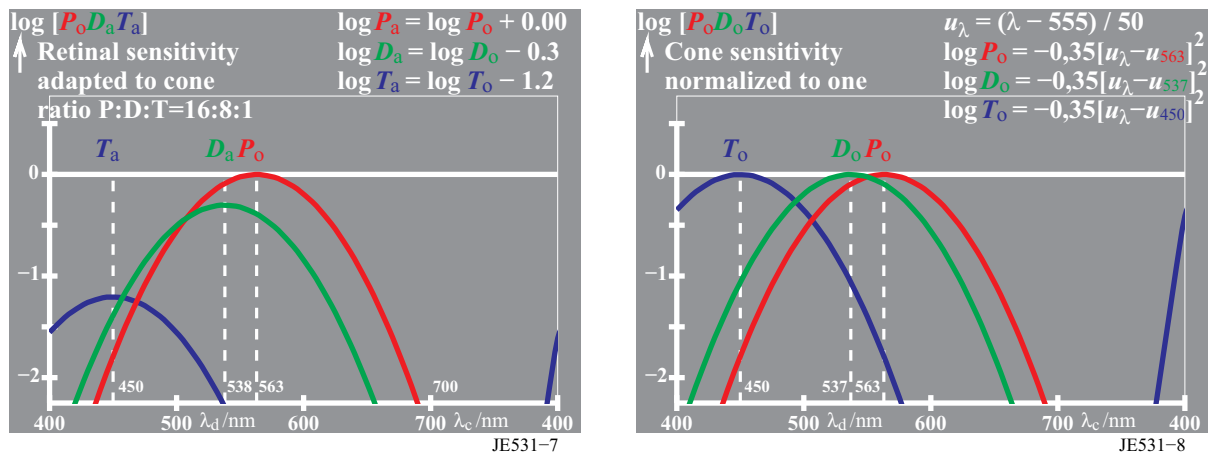


Fig. 11: Log cone sensitivities $P_a(\lambda)$, $D_a(\lambda)$, and $T_a(\lambda)$ normalized to the ratio $P:D:T=16:8:1$ (left), and maxima of $P_0(\lambda)$, $D_0(\lambda)$, and $T_0(\lambda)$ equal on a log scale (right).

Fig. 11 shows the log cone sensitivities $P_a(\lambda)$, $D_a(\lambda)$, and $T_a(\lambda)$ normalized to the ratio $P:D:T=16:8:1$ (left) and with maxima of $P_0(\lambda)$, $D_0(\lambda)$, and $T_0(\lambda)$, all normalized to zero ($\log P, D, T_{\max} = \log 1 = 0$) (right). The differences are straight lines (not shown here). The slope of these lines increases as linear function of the difference of the maxima. If the log sensitivities are normalized to zero then the lines cut the wavelength range in the middle between the two maxima, compare Fig. 16 (right).

6. Sensitivities $P(\lambda)$, $D(\lambda)$, and $T(\lambda)$ and signals $U_0(\lambda)$, $G_0(\lambda)$, $J_0(\lambda)$, $B_0(\lambda)$, and $R_0(\lambda)$

This section is intended to give equations for the calculation of the signals for elementary Green G , Yellow J , Blue B , and Red R as function of wavelength. The calculated signals $U_0(\lambda)$ are similar to $V(\lambda)$. At first there seem to be **no** relation between the cone sensitivities $P_0(\lambda)$, $D_0(\lambda)$, and $T_0(\lambda)$ of Fig. 11 and the signals $G_0(\lambda)$, $J_0(\lambda)$, $B_0(\lambda)$, and $R_0(\lambda)$.

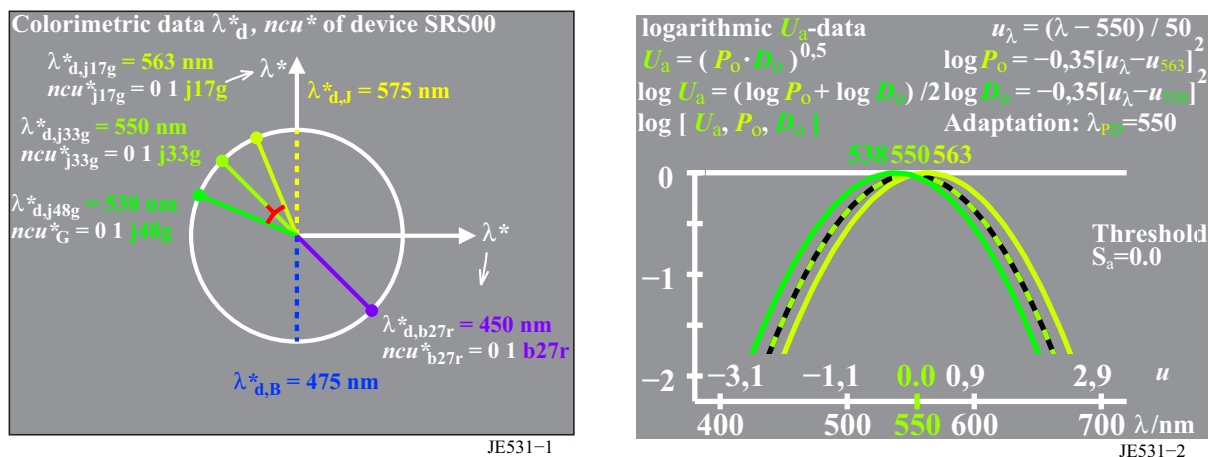


Fig. 12: Two sensitivities $P_0(\lambda)$ and $D_0(\lambda)$ produce signals $U_a(\lambda)$ for monochromatic colours (right) and schematic location in a colour circle with Yellow J on top and Blue B down (left). Fig. 12 shows two sensitivities $P_0(\lambda)$ and $D_0(\lambda)$ which produce signals $U_a(\lambda)$ for monochromatic colours (right) and schematic location in a colour circle with Yellow J on top and Blue B down (left). A red mark indicates how the signals $U_a(\lambda)$ are calculated.

In the following we will clearly distinguish between sensitivities and signals. The model curves for $P_0(\lambda)$, $D_0(\lambda)$, and $T_0(\lambda)$ shown in Fig. 11 are cone sensitivities. Any Figure may use a linear or logarithmic scale. Signals are produced by logarithmic summation or logarithmic differenc-

es. An exception is the $V(\lambda)$ function. $V(\lambda)$ is defined as a sensitivity which is defined as a linear sum of $P_0(\lambda)$ and $D_0(\lambda)$. Fig. 12 (right) uses the logarithmic sum which creates a signal instead of a sensitivity. The difference of the sensitivity (linear sum $V(\lambda)$) and the signal (logarithmic sum $U(\lambda)$) is less than 2% for both on a linear scale compared to the maximum. About 2% is near the achromatic threshold in a white surround. Therefore for applications, if a linear sum is equal to a logarithmic sum to describe the experiments the linear mode is preferred. The CIE has chosen the linear definition of $V(\lambda) = c_1 P_0(\lambda) + c_2 D_0(\lambda)$ which is called the *Abney law* (c_1, c_2 constants). Therefore in the following the sensitivity $V(\lambda)$ and the signals $U_0(\lambda)$ are equal within 2% between 400nm and 700nm. However, for example for $V(\lambda)$ and $T_0(\lambda)$ with top wavelength differences larger than 25 nm (in this case 100 nm), the calculated data by the linear and log formula are very different.

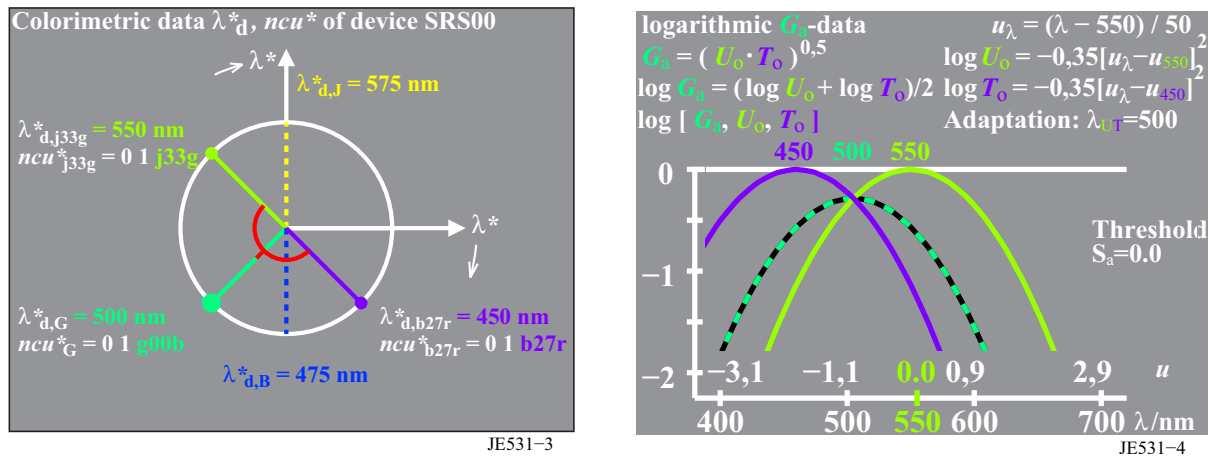


Fig. 13: Two sensitivities $U_0(\lambda)$ and $T_0(\lambda)$ which produce signals $G_a(\lambda)$ for monochromatic colours (right) and schematic location in a colour circle with Yellow J on top and Blue B down (left)

Fig. 13 shows two sensitivities $U_0(\lambda)$ and $T_0(\lambda)$ which produce signals $G_a(\lambda)$ for monochromatic colours (right) and schematic location in a colour circle with Yellow J on top and Blue B down (left). The maximum of $G_a(\lambda)$ his below zero. By a vertical shift a normalization to $G_0(\lambda)$ with the value zero on a log scale is possible. The method is often used in the following, compare also Fig. 11. Again a red mark indicates the components to define the signals $G_a(\lambda)$.

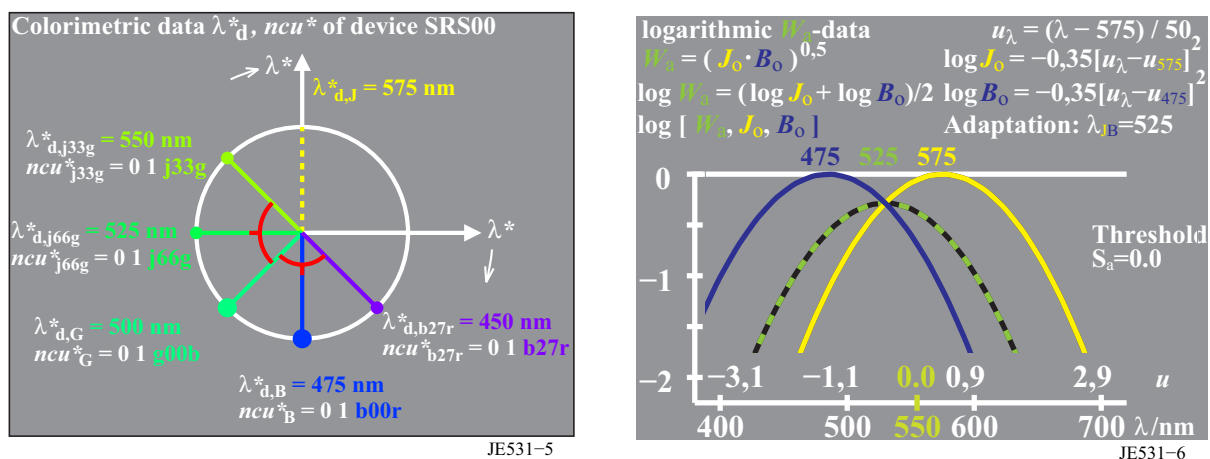


Fig. 14: Two signals $J_0(\lambda)$ and $B_0(\lambda)$ produce signals $W_a(\lambda)$ for monochromatic colours (right) and schematic location in a colour circle with Yellow J on top and Blue B down (left).

Fig. 14 shows that two signals $J_0(\lambda)$ and $B_0(\lambda)$ produce signals $W_a(\lambda)$ for monochromatic colours (right) and schematic location in a colour circle with Yellow J on top and Blue B down

(left). The signals Blue $B_0(\lambda)$ are produced by the mean of the signals of Green $G_0(\lambda)$ and the sensitivity $T_0(\lambda)$.

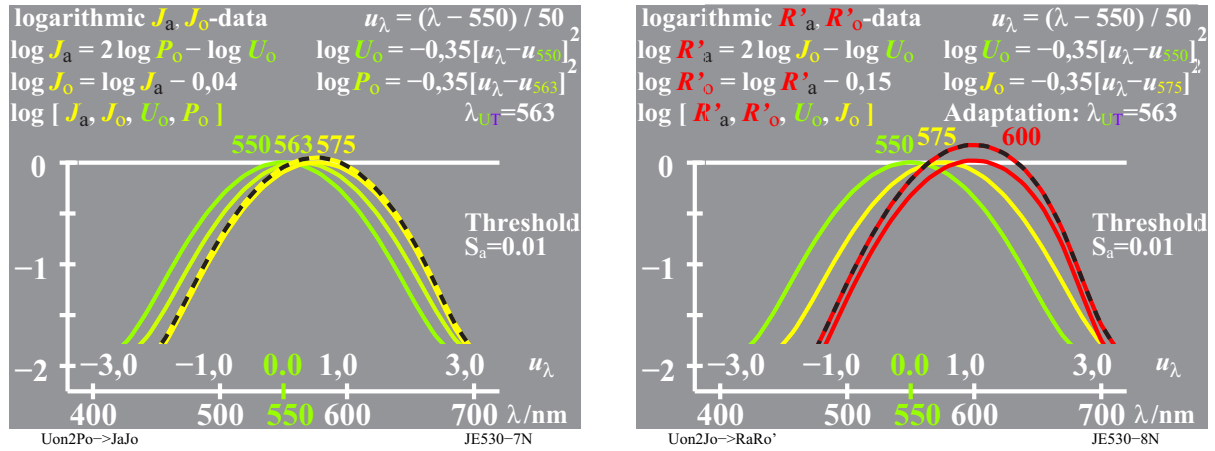


Fig. 15: Signals $J_0(\lambda)$ defined by equations which use the sensitivity $P_0(\lambda)$ and $U_0(\lambda)$ (left) and signals $R_0(\lambda)$ defined by equations which use the sensitivity $U_0(\lambda)$ and the signals $J_0(\lambda)$ (right). Fig. 15 shows the signals $J_0(\lambda)$ defined by equations in the figure which use the sensitivity $P_0(\lambda)$ and $U_0(\lambda)$ (left) and signals $R_0(\lambda)$ defined by equations which use the sensitivity $U_0(\lambda)$ and the signals $J_0(\lambda)$ (right). The equations in Fig. 15 may be called the outer mixture equations compared to the inner mixture equations used in Fig. 12 to 14.

In Fig. 15 an achromatic threshold $S_a=0,01$ is added which is at least 1% of the maximum value for all wavelength. This threshold produces a minimum signal of -2 on a log scale for all wavelength. The threshold 1% is defined by visual experiments. For older people this threshold may increase for example up to 4% by the increased scattering within the eye media.

The shape of the calculated signals, for example $R_0(\lambda)$, deviates from the parable form at both ends of the spectrum. The shape gets smaller and more steep. Fig. 10 shows the sensitivity $T_0(\lambda)$ at the blue end of the spectrum with such a property and the model calculation gives this shape property in agreement with the measurement of the sensitivity of the cone $T(\lambda)$.

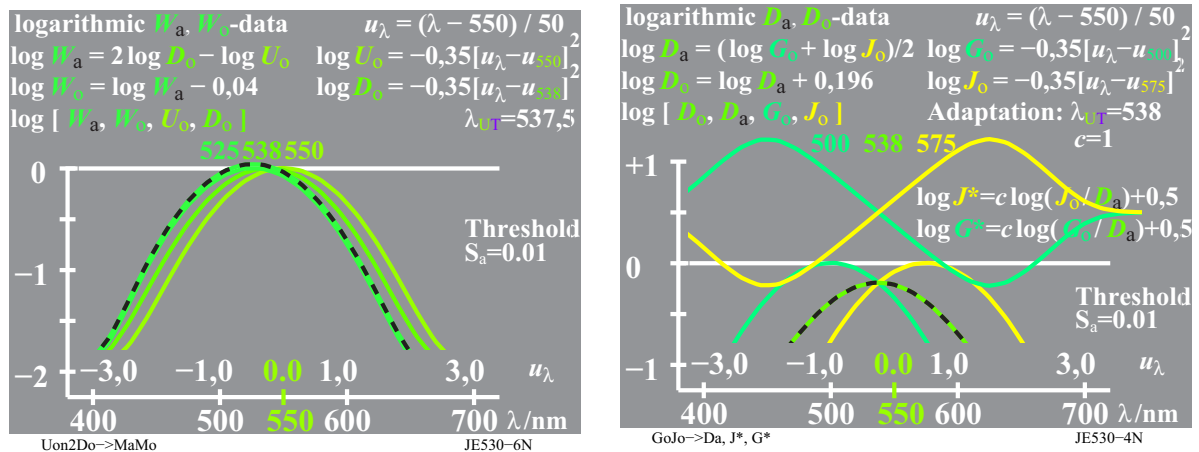


Fig. 16: Signals $W_0(\lambda)$ defined by equations which use the sensitivities $D_0(\lambda)$ and $U_0(\lambda)$ (left) and for example signal differences $\log J_0(\lambda) - \log D_a(\lambda)$ which form a straight line between 500 nm and 575 nm (right).

Fig. 16 shows the signals $W_0(\lambda)$ defined by equations which use the sensitivities $D_0(\lambda)$ and $U_0(\lambda)$ (left) and for example signal differences $\log J_0(\lambda) - \log D_a(\lambda) = \log [J_0(\lambda) / D_0(\lambda)]$ which form a straight line between 500 nm and 575 nm (right). Within the range 500 nm to 575 nm

the Yellowness J^* increases linearly as function of wavelength and the Greenness G^* decreases similar. According to Fig. 16 a yellow-green hue (JG) shall be at the middle wavelength between Green G (500nm) and Yellow J (575nm) and shall be located at $\lambda_d = 537,5$ nm. Experimental data of four visual intermediate hues BR, BG, JG, and JR are for example defined in the elementary hue circle of *Miescher* (1948) for CIE illuminant C. The predictions depend on the location of the dominant wavelength of elementary Green G_o ($\lambda_d = 513$ nm?) and are not discussed here.

7. Improved coordinates of colour vision based on elementary colours

There are linear and nonlinear coordinates of colour vision. Some are defined based on visual experiments, for example $V(\lambda) = y_{\text{bar}}(\lambda)$. The tristimulus value $z_{\text{bar}}(\lambda)$ is similar to the cone absorption $T(\lambda)$. The differences $a_{\text{bar}}(\lambda) = x_{\text{bar}}(\lambda) - y_{\text{bar}}(\lambda)$ and $b_{\text{bar}}(\lambda) = -0,4 [z_{\text{bar}}(\lambda) - y_{\text{bar}}(\lambda)]$ show similarities with the elementary colour coding, compare Fig 4. However, $b_{\text{bar}}(\lambda)$ has a zero value at 500nm instead of 513 nm, so a function $b'_{\text{bar}}(\lambda) = -0,4 [B_o(\lambda) - y_{\text{bar}}(\lambda)]$ with $B_o(\lambda)$ instead of $z_{\text{bar}}(\lambda) = c_3 T_o(\lambda)$ may be more appropriate. This function has a zero value at 513 nm = $[475 + 0,5 (550 - 475)]$ nm. We know that there are some improvements compared to the functions $a_{\text{bar}}(\lambda)$ and $b_{\text{bar}}(\lambda)$ of *Hurvich* and *Jameson* (1955). However, we will still use these CIE functions in the following within a linear colour valence metric and a higher nonlinear colour metric.

color valence metric (color data: linear relation to CIE 1931 data)		
linear color terms	name and relationship to CIE tristimulus or chromaticity values	notes:
luminous value	$Y = y (X + Y + Z)$	
chromatic value	<i>for linear chromatic value diagram (A, B)</i>	
red-green	$A = [X / Y - X_n / Y_n] Y = [a - a_n] Y$ $= [x / y - x_n / y_n] Y$	$n=D65$ (backgr.)
yellow-blue	$B = - 0,4 [Z / Y - Z_n / Y_n] Y = [b - b_n] Y$ $= - 0,4 [z / y - z_n / y_n] Y$	
radial	$C_{ab} = [A^2 + B^2]^{1/2}$	
chromaticity	<i>for (linear) chromaticity diagram (a, b) compare to linear</i>	
red-green	$a = X / Y = x / y$	<i>cone excitation</i>
yellow-blue	$b = - 0,4 [Z / Y] = - 0,4 [z / y]$	$P/(P+D)=L/(L+M)$
radial	$c_{ab} = [(a - a_n)^2 + (b - b_n)^2]^{1/2}$	$T/(P+D)=S/(L+M)$

JE441-7

Figure 17: Coordinates of the lower colour metric and chromaticity coordinates (a, b)
 Figure 17 shows coordinates of the lower colour metric and the chromaticity coordinates (a, b) which have a linear relation to the CIE chromaticity coordinates (x, y). The chromatic values A and B can be calculated by multiplying the luminance factor Y of the sample with the chromaticity difference a of the sample and the background a_n . Additionally the chromaticity a and b can be compared with the saturation $P / (P+D)$ and $T / (P+D)$ of the three receptors P, D and T or L, M , and S according to CIE 171-1:2005. For example in Figure 17 the ratio $Z / Y = z / y = [(I-x-y) / y]$ is similar to the ratio $T / (P+D) = S / (L+M)$.

Higher colormetric (color data: nonlinear relation to CIE 1931 data)		
non linear color terms	name and relationship with tristimulues or chromaticity values	notes
lightness	$L^* = 116 (Y / 100)^{1/3} - 16 \quad (Y > 0,8)$ Approximation: $L^* = 100 (Y / 100)^{1/2,4}$	CIELAB 1976
chroma	<i>non linear transform of chromatic values A and B</i>	
red-green	$a^* = 500 [(X / X_n)^{1/3} - (Y / Y_n)^{1/3}]$ $= 500 (a' - a'_n) Y^{1/3}$	CIELAB 1976 <i>n=D65 (backgr.)</i>
yellow-blue	$b^* = 200 [(Y / Y_n)^{1/3} - (Z / Z_n)^{1/3}]$ $= 500 (b' - b'_n) Y^{1/3}$	CIELAB 1976
radial	$C^*_{ab} = [a^{*2} + b^{*2}]^{1/2}$	
chromaticity	<i>nonlinear transform of chromaticities a=x/y and b=z/y</i>	<i>compare to log cone excitation</i>
red-green	$a' = (1 / X_n)^{1/3} (x / y)^{1/3}$ $= 0,2191 (x / y)^{1/3} \quad \text{for D65}$	$\log[P / (P+D)]$
yellow-blue	$b' = -0,4 (1 / Z_n)^{1/3} (z / y)^{1/3}$ $= -0,08376 (z / y)^{1/3} \quad \text{for D65}$	$= \log[L / (L+M)]$ $\log[T / (P+D)]$
radial	$c'_{ab} = [(a' - a'_n)^2 + (b' - b'_n)^2]^{1/2}$	$= \log[S / (L+M)]$

JE440-7

Figure 18: Coordinates of the higher color metric with non linear (cube root) chromaticity coordinates (a' , b')

Figure 18 shows coordinates of the higher color metric with non linear chromaticity coordinates (a' , b'). The CIELAB chroma data a^* and b^* can be calculated if the lightness L^* (in this case the approximation $Y^{1/3}$) is multiplied by the non linear chromaticity difference a' of the sample and a'_n of the background (n). This is similar compared to the calculation in the CIELUV colour space. In addition the non linear chromaticity coordinates a' and b' are compared with the saturation $\log [P / (P+D)]$ and $\log [T / (P+D)]$. The cube root coordinates $(Z / Y)^{1/3} = (z / y)^{1/3} = [(1-x-y) / y]^{1/3}$ are similar to the “cone coordinates” $\log [T / (P+D)]$.

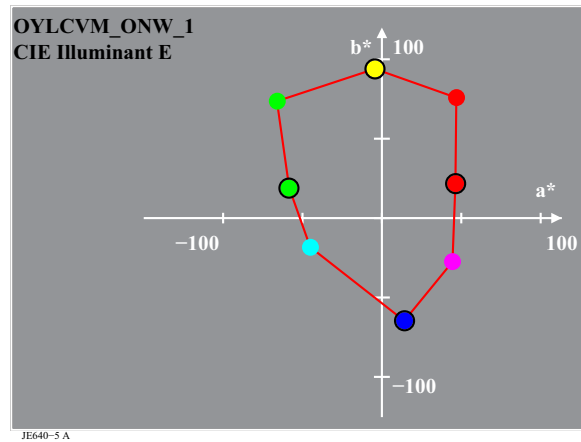
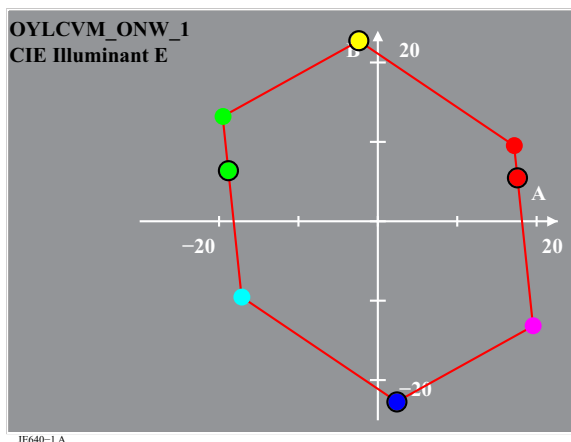


Fig. 19: Optimal colours O_v , L_v , and V_v and complementary colours C_v , M_v , and Y_v in the (A , B) chromatic value diagram and the CIELAB (a^* , b^*) diagram for CIE illuminant E.

Fig. 19 shows the optimal colours O_v , L_v , and V_v and the complementary colours C_v , M_v , and Y_v in the (A , B) chromatic value diagram and the CIELAB (a^* , b^*) diagram for CIE illuminant E.

Fig. A.1 in Annex A shows the CIE data of these colours including $X, Y, Z, x, y, A, B,$ and $L^*, a^*,$ and b^* , and the wavelength range of O_o, L_o, V_o and C_o, M_o, Y_o and elementary colours $R,$ and $G.$

Annex B shows application examples of the developed colorimetric coordinates with the property of equal chromatic moment for complementary optimal colours. Based on the coordinates A and B the equal discrimination measured by *Holtsmark* and *Valberg* (1969) can be described.

However, the CIE coordinates X and Z are not based on direct visual data similar to the device independent coordinates used in image technology. The report CIE R1-47:2009 is important for both areas which may now be based on device independent *relative* coordinates. However, the metric for the discrimination is still open. At threshold the colour metric may be linear and for large colour differences non linear similar as included in CIELAB. Fig. 17 show the linear chromaticity (a, b) and Fig. 18 the cube root chromaticity (a', b') which is used to calculate the CIE-LAB coordinates (a^*, b^*) above threshold ($X, Z, Y > 1$), and compared to White W (X, Z, Y near 100).

8. Elementary optimal colours Red R_o and Green G_o

The *optimal* colours Blue B_o and Yellow J_o which divide the spectrum near 513nm are complementary and mix to white W . In addition the two *monochromatic* colours Blue B_o and Yellow J_o with the dominant wavelength $\lambda_d = 475\text{nm}$ and 575nm mix two white and are on a line in the CIE (x, y) chromaticity diagram.

The optimal colours which are expected according to *Hurvich* and *Jameson* (1955) as Green G_o and Red R_o divide the spectrum in the range between 475nm and 575nm and the rest are complementary and mix to white W . However the optimal colour G_o with the dominant wavelength $\lambda_d = 525\text{nm}$ appears yellowish green and Red R_o with the dominant wavelength $\lambda_c = 525\text{nm}$ (on the purple line) appears bluish red. Both appear therefore not as elementary colours.

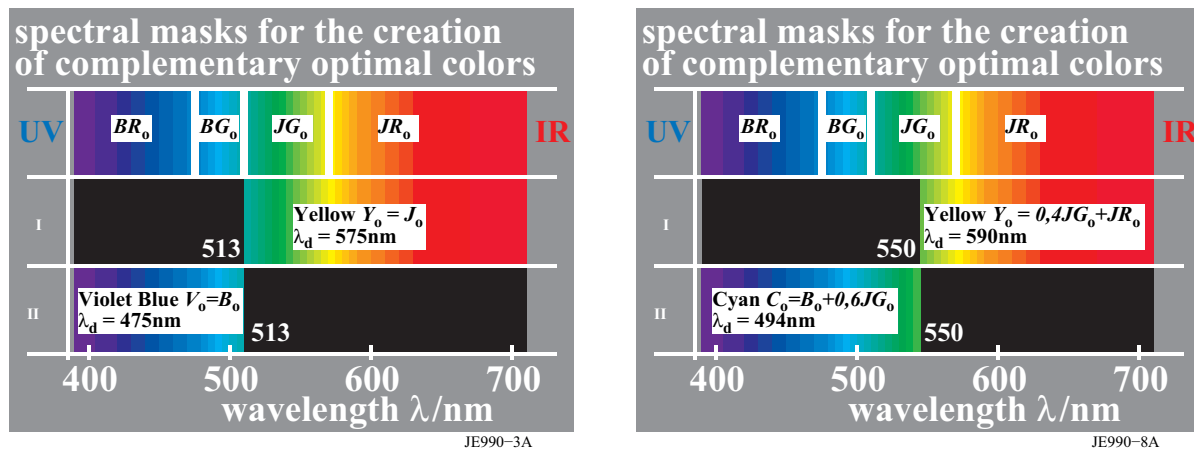


Fig. 20: Complementary optimal colours pairs which divide the spectrum near 513nm and 550nm

Fig. 20 shows the complementary optimal colours Blue B_o and Yellow J_o which divide the spectrum at $\lambda_d = 513\text{nm}$ (*left*). This division is based on the elementary colour Green G_o . CIE R1-47:2009 has defined this colour as CIE-test colour no. 11 with approximately the dominant wavelength $\lambda_d = 513\text{nm}$. Fig. 20 shows the complementary optimal colours Cyan blue C_o and Yellow Y_o which divide the spectrum at $\lambda_d = 550\text{nm}$ (*right*). This division based on the $V(\lambda)$ function with a maximum near 550nm. This wavelength limit is used in the following as one wavelength limit to define an elementary optimal Green G_o .

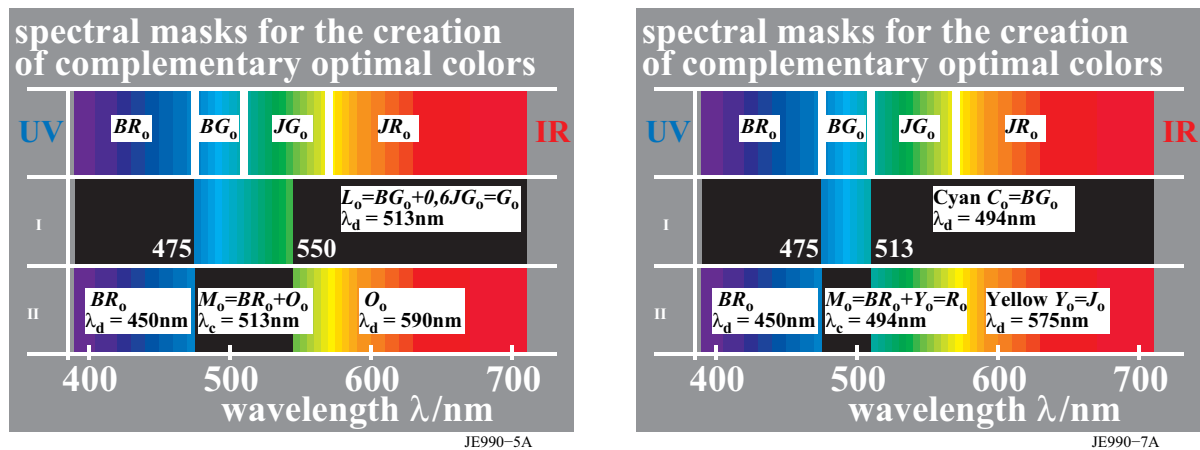


Fig. 21: Wavelength limits 475, 513 and 550 nm to define a special elementary optimal Green G_o and elementary Red R_o .

Fig. 21 shows the wavelength limits 475, 513 and 550 nm to define a special elementary optimal Green G_o and elementary Red R_o . A special elementary Green G_o (left) is defined by the limits 475nm (dominant wavelength of elementary Blue B_o) and 550nm (maximum of $V(\lambda)$).

A special elementary Red R_o (right) is defined by the limits 513nm (dominant wavelength of elementary Green G_o) and 475nm (dominant wavelength of elementary Blue B_o). This broad band elementary Red $R_o = BR_o + J_o$ is complementary to Cyan blue $C_o = BG_o$.

At the moment there is no explanation why these optimal colours with these wavelength limits appear elementary Green G_o and elementary Red R_o . But we know that the model of *Hurvich* and *Jameson* with the wavelength limits 475nm and 575nm for both fails. In addition we realize large similarities to image technology with approximately the colours O (orange red) - W - C and colours L (leaf green) - W - M on a line in the CIE (x,y) chromaticity diagram, compare Fig. 5

9. Summary

The report CIE R1-47 “Hue Angles of Elementary Colours” which proposes the CIE-test colours no. 9 to 12 of CIE 13.3 “Colour Rendering” as Elementary Colours Red R , Yellow J , Green G and Blue B is used to define optimal elementary colours Red R_o , Yellow J_o , Green G_o and Blue B_o . Many relations of these four *elementary* colours and the six *device* colours *OYLCVM* of image technology are given and discussed. The relation to the cone sensitivities *PDT* or *LMS* according to CIE 179-1:2006 is discussed. Elementary colour coordinates are given which produce a hexagon in a chromatic value diagram (A, B) . The diagram (A, B) has a symmetry compared to the origin (white) for any CIE illuminant. This property of the coordinates A and B and the radial chromatic value C is the basis to describe the equal threshold for complementary optimal colours published by *Holtsmark* and *Valberg* (1969).

Acknowledgment

In thank Prof. Dr. Johannes Grebe-Ellis, the owner of the web site

<http://www.experimentum-lucis.de>

for the permission to use a figure of this web site as Fig. 1 in this paper.

9. References

CIE 13.3:1995, Method of measuring and specifying colour rendering of light sources.

CIE 15: 2004, Colorimetry, 3rd edition.

CIE 170-1:2006, Fundamental chromaticity diagram with physiological axes - Part 1.

Hurvich, L.M. (1981), Colour vision, Sinauer Associates Inc. Massach., ISBN 0-87893-337-9.

ISO/IEC 15775:1999, Information Technology – Office Systems – Method for specifying image reproduction of colour copying machines by analog test charts - Realisation and application.

Melgosa, Manuel (2009), Correspondence after the 2009 meeting of CIE TC1-63 with figures showing a large increase of Stress near threshold (0,3 to 1,0 CIELAB) for many data sets.

Miescher, K. (1948) Neuermittlung der Urfarben und deren Bedeutung fuer die Farbordnung, Helv. Physiol. Acta 6, C12-C13

Miescher, K. (1969), The natural colour conception serving as base for elementary colour teaching, AIC Colour 69, Stockholm, Musterschmidt, p. 1231-1241

Natural Colour System NCS (1982), Svensk Standard SS 01 91 0:1982, Colour notation system – SS 01 91 01:1982, CIE tristimulus values and trichromatic co-ordinates for some 16 000 colour notations according to SS 01 91 00 – SS 01 91 02:1982, Colour atlas – SS 01 91 02:1982, CIE tristimulus values and chromaticity co-ordinates for samples in SS 01 91 02

Richter, K. (1980), Cube root color spaces and chromatic adaptation, Color Res. and Appl. 5, no. 1, pp. 25-43

Richter, K. (1996), Computergrafik und Farbmeterik, Farbsysteme, PostScript, geräteunabhängige CIE-Farben, VDE-Verlag, Berlin, ISBN 3-8007-1775-1, 288 pages including CD-ROM and about 500 pictures in colour, see

<http://www.ps.bam.de/buche>

Richter, K. (2003), Basic data, methods and formula to bridge the gap for color differences between large CIELAB color differences, e.g. $\Delta E^*_{ab}=20$, and threshold differences for office conditions, see 14 pages, 1 MB, <http://www.ps.bam.de/CIE6303B.PDF>

Richter, K. (2006), Device dependent linear relative CIELAB data lab* and colorimetric data for corresponding colour input and output on monitors and printers, CIE Symposium, 75 years colorimetric observer, Ottawa/Canada, CIE x030:2006, 129-135

Richter, K. (2008), Colorimetric model of logarithmic colour spaces LMSLAB, Part II, The Proceedings of the 26th Session of the CIE, 2007, Beijing, Proceedings Volume 2.pdf, 199-230

Holtsmark, T. and Valberg, A. (1969), Colour discrimination and hue, Nature, Volume 224, October 25, S. 366-367

Valberg, A. and Holtsmark, T. (1971), Similarity between JND-curves for complementary optimal colours, In: Color Metrics, AIC, Soesterberg, TNO, 58-68

Valberg, A. (2005), Light Vision Color, John Wiley & Sons, ISBN 0-470-84903-7, 462 pages.

Author and address: Prof. Dr. Klaus Richter, Berlin University of Technology,

Walterhoferstrasse 44, 14165 Berlin, Germany

Tel. +49 30 84 50 90 38, Fax -84 50 90 40,

email: klaus.richter@mac.com

internet:

<http://130.149.60.45/~farbmeterik> and

<http://web.me.com/klaus.richter>

For recent publications see <http://130.149.60.45/~farbmeterik/XY91FEN.html>

Annex A: CIE data of six optimal colours *OYLCVM* including symmetry for (*A*, *B*) data

This Annex A shows the CIE data including *X*, *Y*, *Z*, *x*, *y*, *A*, *B*, and *L**, *a**, and *b**, and the wavelength range of *optimal colours* *O_o*, *L_o*, *V_o*, and *C_o*, *M_o*, *Y_o*, and the *elementary colours* *R*, *G*.

<i>X</i>	<i>Y</i>	<i>Z</i>	<i>x</i>	<i>y</i>	<i>A</i>	<i>B</i>	<i>Cr</i>	<i>a</i>	<i>b</i>	<i>c</i>	<i>L*</i>	<i>a*</i>	<i>b*</i>	<i>C*ab</i>	<i>a'</i>	<i>b'</i>	<i>c'</i>	<i>OYLCVM_ONW_1</i>	
CIE Illuminant E																			
61.4	35.7	0.0	0.632	0.367	25.7	14.2	29.4	0.71	0.39	0.82	66.3	70.3	113.7	133.7	0.258	-0.008	0.258	0.0	00 575_770
83.1	86.7	1.5	0.485	0.505	-3.5	34.0	34.2	-0.04	0.39	0.39	94.6	-6.6	140.9	141.1	0.212	-0.022	0.213	0.0	01 515_770
21.6	50.9	1.5	0.292	0.687	-29.3	19.7	35.3	-0.57	0.38	0.69	76.6	-99.1	110.4	148.3	0.161	-0.026	0.164	0.0	02 515_770
26.7	54.9	31.0	0.237	0.487	-28.2	9.5	29.8	-0.51	0.17	0.54	79.0	-87.5	28.4	92.0	0.169	-0.071	0.183	0.0	03 0.70*L+0,30*C
38.5	64.2	99.9	0.189	0.316	-25.7	-14.2	29.4	-0.4	-0.22	0.45	84.0	-67.6	-27.3	73.0	0.181	-0.099	0.207	0.0	04 380_575
16.8	13.2	98.4	0.13	0.103	3.5	-34.0	34.2	0.26	-2.57	2.58	43.1	21.1	-96.9	99.2	0.233	-0.168	0.287	0.0	05 380_515
78.3	49.0	98.4	0.346	0.217	29.3	-19.7	35.3	0.59	-0.4	0.72	75.4	66.6	-41.3	78.4	0.251	-0.108	0.274	0.0	06 380_515+575_770
64.5	38.1	17.7	0.535	0.316	26.3	8.1	27.6	0.69	0.21	0.72	68.1	69.4	32.6	76.7	0.256	-0.066	0.265	0.0	07 0.18*M+0,82*O
61.4	35.7	0.0	0.632	0.367	25.7	14.2	29.4	0.71	0.39	0.82	66.3	70.3	113.7	133.7	0.258	-0.008	0.258	0.0	08 575_770
0.1	0.1	0.1	0.332	0.332	0.0	0.0	0.0	0.0	0.0	0.0	0.9	0.0	0.0	0.0	0.215	-0.086	0.232	0.0	09 380_770
100.0	100.0	100.0	0.333	0.333	0.0	0.0	0.0	0.0	0.0	0.0	100.0	0.0	0.0	0.0	0.215	-0.086	0.232	0.0	10 380_770
CIE Standard Illuminant D65																			
54.8	32.3	0.0	0.628	0.37	24.1	14.0	27.9	0.74	0.43	0.86	63.6	73.0	109.1	131.3	0.249	-0.008	0.249	0.0	00 575_770
76.8	85.2	1.6	0.469	0.52	-4.1	36.4	36.7	-0.04	0.42	0.43	94.0	-8.2	140.2	140.5	0.202	-0.028	0.203	0.0	01 515_770
22.0	52.9	1.6	0.288	0.69	-28.2	22.4	36.0	-0.53	0.42	0.68	77.8	-97.1	112.7	148.8	0.156	-0.026	0.158	0.0	02 515_770
27.5	57.3	33.7	0.231	0.483	-27.0	11.4	29.3	-0.47	0.2	0.51	80.3	-84.6	30.8	90.1	0.163	-0.07	0.178	0.0	03 0.70*L+0,30*C
40.2	67.6	108.8	0.185	0.312	-24.1	-14.0	27.9	-0.35	-0.2	0.41	85.8	-63.5	-24.3	68.1	0.176	-0.098	0.201	0.0	04 380_575
18.1	14.7	107.2	0.129	0.105	4.1	-36.4	36.7	0.28	-2.47	2.49	45.2	23.9	-93.3	96.4	0.224	-0.162	0.277	0.0	05 380_515
72.9	47.0	107.2	0.321	0.206	28.2	-22.4	36.0	0.6	-0.47	0.76	74.2	68.9	-43.4	81.5	0.242	-0.11	0.266	0.0	06 380_515+575_770
58.0	34.9	19.3	0.516	0.311	24.8	7.4	25.9	0.71	0.21	0.74	65.7	72.0	26.4	77.4	0.248	-0.068	0.257	0.0	07 0.18*M+0,82*O
54.8	32.3	0.0	0.628	0.37	24.1	14.0	27.9	0.74	0.43	0.86	63.6	73.0	109.1	131.3	0.249	-0.008	0.249	0.0	08 575_770
0.0	0.1	0.1	0.311	0.327	0.0	0.0	0.0	0.0	0.0	0.0	0.9	0.0	0.0	0.0	0.205	-0.086	0.223	0.0	09 380_770
95.0	100.0	108.8	0.312	0.329	0.0	0.0	0.0	0.0	0.0	0.0	100.0	0.0	0.0	0.0	0.205	-0.086	0.223	0.0	10 380_770
CIE Illuminant D50																			
60.9	35.4	0.0	0.632	0.367	26.8	11.6	29.2	0.75	0.32	0.82	66.0	75.4	113.1	135.9	0.275	-0.009	0.275	0.0	00 575_770
82.9	87.3	1.5	0.482	0.508	-1.2	28.1	28.2	-0.01	0.32	0.32	94.8	-2.3	137.9	137.9	0.225	-0.023	0.227	0.0	01 515_770
22.0	51.9	1.5	0.291	0.688	-28.0	16.5	32.5	-0.54	0.31	0.62	77.2	-96.2	107.9	144.6	0.172	-0.028	0.174	0.0	02 515_770
26.0	55.7	25.7	0.242	0.518	-27.6	8.0	28.8	-0.49	0.14	0.51	79.4	-88.2	28.8	92.8	0.178	-0.071	0.191	0.0	03 0.70*L+0,30*C
35.4	64.5	82.4	0.194	0.353	-26.8	-11.6	29.2	-0.41	-0.18	0.45	84.2	-73.9	-27.0	78.7	0.188	-0.099	0.212	0.0	04 380_575
13.4	12.6	80.9	0.125	0.118	1.2	-28.1	28.2	0.09	-2.22	2.22	42.2	8.1	-98.3	98.6	0.234	-0.17	0.289	0.0	05 380_515
74.4	48.0	80.9	0.365	0.236	28.0	-16.5	32.5	0.58	-0.34	0.67	74.8	66.9	-42.1	79.0	0.265	-0.109	0.287	0.0	06 380_515+575_770
63.3	37.6	14.6	0.547	0.325	27.0	6.5	27.8	0.71	0.17	0.73	67.7	73.5	32.1	80.3	0.273	-0.066	0.281	0.0	07 0.18*M+0,82*O
60.9	35.4	0.0	0.632	0.367	26.8	11.6	29.2	0.75	0.32	0.82	66.0	75.4	113.1	135.9	0.275	-0.009	0.275	0.0	08 575_770
0.0	0.0	0.0	0.344	0.357	0.0	0.0	0.0	0.0	0.0	0.0	0.9	0.0	0.0	0.0	0.226	-0.086	0.242	0.0	09 380_770
96.4	100.0	82.4	0.345	0.358	0.0	0.0	0.0	0.0	0.0	0.0	100.0	0.0	0.0	0.0	0.226	-0.086	0.242	0.0	10 380_770
CIE Standard Illuminant A																			
83.5	46.7	0.0	0.64	0.358	32.1	6.6	32.8	0.68	0.14	0.7	74.0	68.2	125.5	142.9	0.368	-0.012	0.369	0.0	00 575_770
104.3	92.5	1.2	0.526	0.467	2.7	12.6	12.9	0.02	0.13	0.14	97.0	4.2	130.1	130.2	0.316	-0.028	0.317	0.0	01 515_770
20.8	45.8	1.1	0.307	0.675	-29.4	6.0	30.0	-0.64	0.13	0.65	73.4	-97.9	90.3	133.2	0.233	-0.035	0.236	0.0	02 515_770
22.5	48.0	11.4	0.274	0.585	-22.2	2.2	30.3	-0.62	0.04	0.63	74.8	-96.7	19.5	98.7	0.236	-0.075	0.247	0.0	03 0.70*L+0,30*C
26.3	53.2	35.5	0.228	0.462	-32.1	-6.6	32.8	-0.6	-0.12	0.61	78.0	-94.6	-37.8	101.9	0.24	-0.106	0.262	0.0	04 380_575
5.4	7.4	34.3	0.115	0.157	-2.7	-12.6	12.9	-0.36	-1.7	1.74	32.7	-26.3	-113.6	116.6	0.274	-0.202	0.341	0.0	05 380_515
88.9	54.1	34.4	0.501	0.305	29.4	-6.0	30.0	0.54	-0.11	0.55	78.5	58.4	-34.7	67.9	0.358	-0.104	0.373	0.0	06 380_515+575_770
84.4	48.0	6.2	0.608	0.346	31.6	4.3	31.9	0.65	0.09	0.66	74.8	66.3	44.7	80.0	0.366	-0.061	0.371	0.0	07 0.18*M+0,82*O
83.5	46.7	0.0	0.64	0.358	32.1	6.6	32.8	0.68	0.14	0.7	74.0	68.2	125.5	142.9	0.368	-0.012	0.369	0.0	08 575_770
0.1	0.0	0.0	0.445	0.405	0.0	0.0	0.0	0.0	0.0	0.0	0.9	0.0	0.0	0.0	0.313	-0.086	0.325	0.0	09 380_770
109.8	99.9	35.5	0.447	0.407	0.0	0.0	0.0	0.0	0.0	0.0	100.0	0.0	0.0	0.0	0.313	-0.086	0.325	0.0	10 380_770

$$A = [(X/X_n) - (Y/Y_n)]Y \quad B = -0.4[(Z/Z_n) - (Y/Y_n)]Y \quad a = X/Y = x/y \quad b = -0.4Z/Y = -0.4z/y \quad (X, Y, Z \geq 0.89)$$

$$a^* = 500 [(X/X_n)^{1/3} - (Y/Y_n)^{1/3}] \quad b^* = 200 [(Y/Y_n)^{1/3} - (Z/Z_n)^{1/3}] \quad a' = (1/X_n)^{1/3} (x/y)^{1/3} \quad b' = -0.4(1/Z_n)^{1/3} (z/y)^{1/3}$$

$$= 500 (a' - a_n) Y^{1/3} \quad = 500 (b' - b_n) Y^{1/3} \quad = 0.2191 (x/y)^{1/3} \quad = -0.08376 (z/y)^{1/3} \quad \text{CIE LAB for } n=D65$$

Fig. A.1: CIE data of six optimal colours *OYLCVM* including colour names and spectral range, for example $O_0 = JR_0 = 575_770$ nm. The data are given for the CIE standard illuminants D65 and A and the CIE illuminants E and D50. Some of the equations of Fig. 17 and 18 are repeated. Fig. 19 shows the data set in the CIE diagrams (*A*, *B*) and (*a**, *b**) for CIE illuminant E. The six optimal colours *OYLCVM* define a triangle in the CIE chromaticity diagram (*x*, *y*), compare Fig. 5. The six optimal colours *OYLCVM* define a chromatic value hexagon (*A*, *B*) which is point symmetric compared to the origin, and a non regular hexagon (*a**, *b**) of CIELAB, see Fig. 19. The symmetry of the chromatic value hexagon data is the basis for the description of the equal colour difference of complementary optimal colours, compare section 2 and Annex B and Annex C.

Annex B: Equations and possible metric to describe achromatic and chromatic thresholds

In this annex B the linear equations in Fig. 17 are used for the description of the *Holtsmark-Valberg* experiments. The red-green chromatic value for the basic colour is

$$A = (a - a_n) Y = (x/y - x_n/y_n) Y \quad (\text{B};1)$$

Then it is valid with the normalization of image technology for the range 0 to 1 (Index 01)

$$A_{01} = (a_{01} - a_{01n}) Y_{01} = (x_{01}/y_{01} - 1) Y_{01} = (X_{01}/Y_{01} - 1) Y_{01} = X_{01} - Y_{01}$$

For the complementary colours it is always valid

$$X_{01c} = 1 - X_{01}, \quad Y_{01c} = 1 - Y_{01}, \quad Z_{01c} = 1 - Z_{01}$$

Therefore

$$A_{01c} = X_{01c} - Y_{01c} = 1 - X_{01} - (1 - Y_{01}) = Y_{01} - X_{01} = -A_{01} \quad (\text{B};2)$$

If we use the three-dimensional difference in the linear space, then we have for the basic colours at threshold (th)

$$\text{delta } E^*_{\text{ABY,th}} = \{ [\text{delta } A_{01}]^2 + [\text{delta } B_{01}]^2 + [\text{delta } Y_{01}]^2 \}^{1/2} \quad (\text{B};3)$$

and for the complementary colours at threshold

$$\text{delta } E^*_{\text{ABY,th,c}} = \{ [\text{delta } A_{01c}]^2 + [\text{delta } B_{01c}]^2 + [\text{delta } Y_{01c}]^2 \}^{1/2} \quad (\text{B};4)$$

The absolute hue discrimination is for the complementary optimal colours the same because of equation (B;2)

$$A_{01c} = A_{01} \quad \text{and} \quad B_{01c} = B_{01} \quad (\text{B};5)$$

The last term delta Y_{01} is for the complementary colours different. If one colour is dark then the complementary is light. By the *Weber-Fechner* law it is valid for the achromatic discrimination along the luminance axis

$$\text{delta } Y_{01} = c_Y Y_{01} \quad (\text{B};6)$$

Therefore the above equations are only a solution for the special case that the luminance threshold is below the hue threshold. This is not always true in the *Holtsmark-Valberg* experiments because they report to see in some regions only a lightness difference. In this case we must look for a possibility to modify the threshold model. We can look at the **contrast sensitivity**

$$Y_{01c} / (\text{delta } Y_{01c}) = Y_{01} / (\text{delta } Y_{01}) \quad (\text{B};7)$$

which is according to the *Weber-Fechner* law the **same for complementary colours**.

So instead of the equation (B;3) the following metric is in **complete agreement with the Holtsmark-Valberg threshold results for complementary optimal colours**

$$\text{delta } E^*_{\text{ABY,th}} = \{ [\text{delta } A_{01}]^2 + [\text{delta } B_{01}]^2 + [(\text{delta } Y_{01}) / Y_{01}]^2 \}^{1/2} \quad (\text{B};8)$$

In the colour space ABY and at threshold this formula will calculate the same value for complementary optimal colours

$$\text{delta } E^*_{\text{ABY,th}} = \text{delta } E^*_{\text{ABY,th,c}} \quad (\text{B};9)$$

Equation (B;8) may be the first equation which describes the surprising results of *Holtsmark-Valberg* for thresholds.

Remark 1: During the AIC-symposium in Soesterberg in 1971 there have been very controversial discussions about the *Holtsmark-Valberg* results.

We must be careful about the interpretation of equation (B;8). This equation does not tell us at the moment how to scale A_{01} . In other words if

$$\text{delta } A_{01} = \text{delta } A_{01c}$$

then it is also valid

$$(\text{delta } A_{01}) / A_{01} = (\text{delta } A_{01c}) / A_{01c}$$

The following speculative **equation for complementary optimal colours**

$$\text{delta } E^*_{\text{ABY,th}} = \{ [(\text{delta } A_{01}) / A_{01}]^2 + [(\text{delta } B_{01}) / B_{01}]^2 + [(\text{delta } Y_{01}) / Y_{01}]^2 \}^{1/2} \quad (\text{B};10)$$

is also in full agreement with the *Holtsmark-Valberg* results.

Equations (B;8) and (B;10) are basic steps for the understanding. Many other experimental results on thresholds will help us to come to an improved solution for the description of threshold data and probably scaling data.

Annex C: Line element to describe achromatic and chromatic thresholds

In this annex C line elements of *Helmholtz (1896)* and *Stiles (1946)* are shown. Then some possible equations for line elements to describe the *Holtmark-Valberg* results are given for consideration.

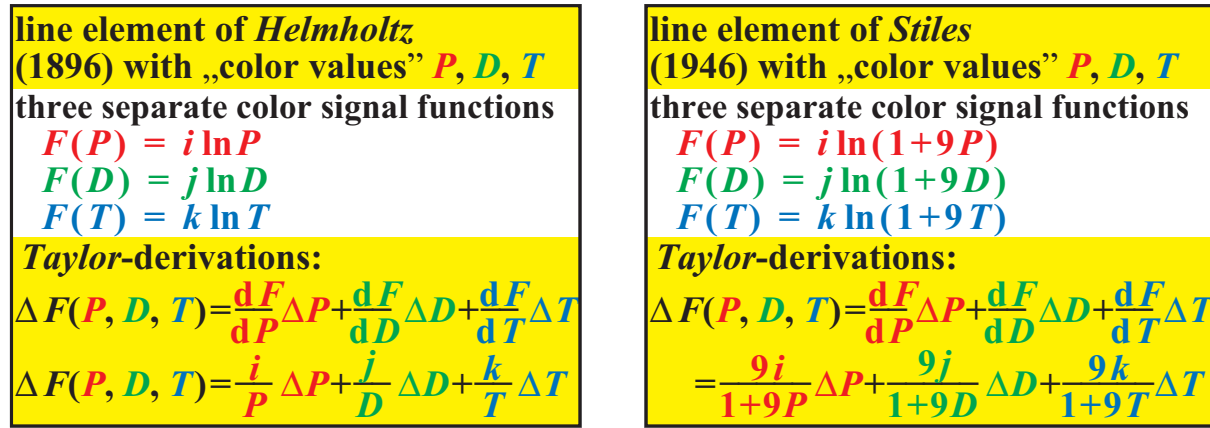


Fig. C.1: Line elements of *Helmholtz (left)* and *Stiles (right)*

Fig. C.1 shows line elements of *Helmholtz (1896, left)* and *Stiles (1946, right)*. The *Weber-Fechner* law $dY/Y = \text{const}$ is similar to the *Helmholtz* line element, for example $dP/P = \text{const}$.

Some mathematics which may be useful to create a line element for threshold data

1. Line element as function of the luminance factor Y.

We calculate the deviation of the following threshold function Q^*_Y which depends only on the luminance factor Y

$$Q^*_Y = \text{const} \ln(1 + c_Y Y)$$

$$dQ^*_Y / dY = \text{const} / (1 + c_Y Y)$$

for $dQ^*_Y = \text{const}$:

$$dY = \text{const} (1 + c_Y Y)$$

Remark: For $c_Y Y \gg 1$ we get the *Weber-Fechner* law: $dY/Y = \text{const}$

2. Line element as function of chromatic value A

We calculate the deviation of the following threshold function Q^*_A which depends only on chromatic value A

$$Q^*_A = \text{const} \ln(1 + c_A A)$$

$$dQ^*_A / dA = \text{const} / (1 + c_A A) \quad \text{for } dQ^*_A = \text{const}:$$

$$dA = \text{const} (1 + c_A A)$$

Remark: For $c_A A \gg 1$ we get (a possible new relation): $dA/A = \text{const}$

3. Line element as function of both chromaticity a and luminance factor Y

We calculate the deviation of the following threshold function Q^*_{aY} which depends on both chromaticity a and luminance factor Y

$$Q^*_{aY} = \text{const} \ln(1 + c_{aY} a Y)$$

$$dQ^*_{aY} / da = \text{const} Y / (1 + c_{aY} a Y)$$

$$dQ^*_{aY} / dY = \text{const} a / (1 + c_{aY} a Y)$$

for $dQ^*_{aY} = \text{const}$ and the deviation to the chromaticity a

$$da = \text{const} (1 + c_A a Y) / Y$$

Remark: For $c_A a Y \gg 1$ we get (a possible new relation) $da Y / (a Y) = da / a = \text{const}$

for $dQ^*_{aY} = \text{const}$ and the deviation to the luminance factor Y

$$dY = \text{const} (1 + c_A a Y) / a$$

Remark: For $c_A a Y \gg 1$ we get the *Weber-Fechner* law

$$dY/Y = \text{const}$$